CuO_x sitting on titanium silicate (ETS-10): influence of copper loading on dispersion and redox properties in relation to de-NO_x activity

Antonella Gervasini * and Paolo Carniti

Dipartimento di Chimica Fisica ed Elettrochimica, Università degli Studi di Milano, Via Camillo Golgi 19, I-20133 Milano, Italy

Received 5 June 2002; accepted 3 September 2002

A series of copper-based catalysts prepared by dispersing the CuO phase on a titanium silicate (ETS-10) crystalline matrix were studied towards their de-NO_x activity. The copper concentration ranged from 0.7 to 70 $atom_{Cu}\,nm^{-2}$, corresponding to 3–18 wt%. The activity of NO reduction with ethylene was related to morphological and chemical properties of the catalysts. The crystalline character of the catalysts possessing high internal surface and microporosity was preserved up to *ca.* 3 $atom_{Cu}\,nm^{-2}$. At higher copper concentration, structure collapse was observed with formation of large aggregates of CuO_x. Temperature-programmed reduction experiments showed two reduction peaks with maximum temperatures at *ca.* 470 and 560 K, for catalysts with copper concentration up to 3.5 $atom_{Cu}\,nm^{-2}$. The two peaks corresponded to the reduction of highly dispersed and non-interacting CuO_x species (470 K) and of crystalline CuO_x species (560 K). Catalysts containing copper at higher concentration had only the high-temperature reduction peak, indicating the presence of large aggregates of CuO_x. All the results collected seem basically consistent with a value of about 2.5–3 $atom_{Cu}\,nm^{-2}$ for the maximum dispersion capacity of CuO on the ETS-10 matrix. The amount of copper deposited on ETS-10 affects the activity of catalysts towards NO reduction. The turnover frequencies per copper site calculated as a function of copper concentration showed a clear decreasing trend starting from 0.7 to 3.5 $atom_{Cu}\,nm^{-2}$. Catalysts with higher copper concentration were completely inactive towards NO reduction.

KEY WORDS: CuO/ETS-10 catalysts; redox properties; NO reduction.

1. Introduction

Copper-containing crystalline or amorphous catalysts have received a great deal of attention in these past years because of their active role in catalytic reactions, considered as potential ways for the abatement of major air pollutants [1–3].

Nitrogen oxide (NO_x) emissions from lean exhaust gas streams originated by stationary and mobile sources are important pollutants that damage the ecosystem. Concerning the issue of NO_x abatement, catalytic conversion of pollutant NO_x into N_2 can be pursued mainly by two methods: NO_x direct decomposition and NO_x selective catalytic reduction with hydrocarbons (SCR-HC). The first one should be the best way to follow, but the high activity of most catalysts in oxygen-free conditions strongly decreases in high-oxygen-containing atmospheres, while the catalyst performance of the second method is enhanced by the presence of oxygen [4–6].

Currently, CuMFI zeolites are among the most studied materials since the early work of Iwamoto *et al.* showed high turnover rates for the NO decomposition and NO reduction [7]. Copper-loaded zeolites of other different structures have been reported to possess interesting SCR activity [8,9]. Unfortunately, severe deactivation in the use of zeolite-based catalysts in real conditions, due mainly to de-alumination and structural collapse, limits their use. As with zeolites, SCR by novel zeolite-like structures loaded with transition metal ions is a rich field for exploitation [10–12].

A number of new crystalline microporous titanosilicate materials have been recently synthesized starting from the discovery of titanium silicalite-1 possessing high-performance oxidation properties. ETS-10 is among the best-known of the titanosilicates containing octahedrally-coordinated Ti(IV) [13]. The six-fold coordination environment renders this titanosilicate inactive as an oxidation catalyst, but still possessing interesting acidity, molecular sieving properties, and high ion-exchange capacity [14]. Aimed at finding new applications for this microporous material, ETS-10 was used as a matrix for dispersing copper ions, leading to a novel catalytic system used in the SCR of NO, as recently reported in the literature. Among others, Gervasini and coworkers [15,16] and Bordiga *et al.* [17] have comparatively studied the ETS-10 and different zeolitic structures with deposition of various amounts of copper by mainly adsorption-calorimetric and spectroscopic studies, respectively. The quantity of copper that may be introduced into the ETS-10 structure at exchangeable sites is determined by the concentration of Ti atoms present in the framework. In over-exchanged

* To whom correspondence should be addressed.
E-mail: antonella.gervasini@unimi.it

1011-372X/02/1200-0235/0

samples, not all the copper is located at exchangeable sites in the structure channels but a fraction of the copper can form copper oxide particles (CuO_x phase) upon calcination on the catalyst surface. Therefore, depending on the loading, different copper species may be co-present, that is, isolated copper ions, small clusters of copper oxides, hydroxides or mixed copper oxide–hydroxide entities, as known on various crystalline matrixes [18–25]. The exact nature of the copper active sites for SCR of NO is still unknown. In fact, both completely exchanged and excessively copper-loaded catalysts in various zeolite structures are claimed to be very active in NO conversion to N_2 [26–29]. Recent results seems to confirm that SCR activity depends on dispersion, envisaging a correlation between the NO reduction rate and the concentration of isolated copper species [19,28–31]. Copper concentration expressed in terms of Cu atoms per catalyst surface unit is nowadays used in the literature as a parameter related to dispersion of copper [32–34]. Centi *et al.* [33] found that on CuO_x/Al_2O_3, NO conversion increased with Cu content up to about 3 $atom_{Cu}\,nm^{-2}$ and for higher Cu content (up to about 6 $atom_{Cu}\,nm^{-2}$) conversion increased to a lesser extent as CuO particles of increasing size were formed. On CuO_x/ZrO_2 catalysts, Indovina and co-workers [32] showed that the rate for activity of NO reduction with NH_3 was proportional to Cu content up to 2.5 $atom_{Cu}\,nm^{-2}$. This suggested the uniform spreading of Cu(II) species on the zirconia surface and, as Cu content increased, small CuO particles, at first, and then bulky CuO species were also formed.

In this paper we report on the catalytic activity of a series of CuO_x/ETS-10 catalysts with different Cu content previously prepared by adsorption from copper acetate aqueous solutions, with or without a second step of impregnation [15,16]. H_2-TPR experiments were qualitatively and quantitatively performed to control the redox properties and the dispersion of the CuO_x species as a function of the Cu content. Catalytic activity of the CuO_x/ETS-10 samples in the abatement of NO with ethylene in the presence of excess oxygen was studied at different temperatures and times in order to obtain data for a kinetic approach. One of the aims of this study is to find activity–copper dispersion relationships.

2. Experimental

2.1. Catalyst preparation

The samples were prepared by loading different amounts of copper in the 3–18 wt% range on an ETS-10 (titanium silicate from Engelhard) microcrystalline matrix. The starting material was the Na^+/K^+ form of ETS-10, $(Na,K)_2Si_5TiO_{13}$ [13], which displays an ion-exchange capacity of 4 meq/g. Details on the preparation could be found in Ref. [16].

The prepared samples, labeled as Cu(02,03,04,1,2,3)-ETS-10 depending on the copper loading, are presented in table 1.

2.2. Physico-chemical analyzes

The copper contents of all the samples were established by inductive coupled plasma (ICP) analysis after dissolution in aqua regia and HF. The presence of Na was detected in the samples independently of Cu content, while *K* was no longer detected in the samples at high Cu exchange (>50%).

The crystallinity of the materials and the presence of copper oxide were established by collecting X-ray diffractions at room temperature on a Philips PW1877 diffractometer using Cu K_α radiation filtered by Ni ($\lambda = 1.5418$ Å).

The N_2 (Tecnogas, Italy; purity >99.999%) adsorption isotherms were obtained using a Sorptomatic 1900 apparatus (Fisons Instruments), employing a static volumetric technique. Two additional pressure gauges working in the ranges 0–130 Pa and 0–13 kPa were inserted in order to measure more accurately the low-pressure values. The analysis was controlled by a

Table 1
Physico-chemical characteristics of the studied copper ETS-10 materials.

Sample	Cu loading [a]		Exchange (%)	Surface area [b] ($m^2\,g^{-1}$)	Concentration ($atom_{Cu}\,nm^{-2}$)
	(wt%)	(mmol g_{cat}^{-1})			
ETS-10	–	–	–	480	–
Cu02-ETS-10	3.1	0.49	24	396	0.742
Cu03-ETS-10	5.8	0.91	46	394	1.395
Cu04-ETS-10	8.4	1.33	66	394	2.021
Cu1-ETS-10	11.4	1.79	90	307	3.520
Cu2-ETS-10	15.1	2.38	119	51	28.066
Cu3-ETS-10	17.7	2.79	139	23	70.475

[a] Determined by ICP analysis.
[b] Determined by '*t*-plot' approach (Harkins–Jura reference equation).

Table 2
Experimental parameters used for performing the TPR analyses on the copper ETS-10 materials.

Sample	Loading		K[a] (s)	$P = K\beta$[b] (K)
	(mg cat.)	(μmol_{Cu})		
ETS-10	55.51	–	–	–
Cu02-ETS-10	55.75	27.199	28.788	4.798
Cu03-ETS-10	54.84	50.059	52.982	8.830
Cu04-ETS-10	53.09	70.185	74.284	12.381
Cu1-ETS-10	54.59	97.942	103.663	17.277
Cu2-ETS-10	53.77	127.782	135.245	22.541
Cu3-ETS-10	53.90	150.144	158.916	26.486

[a] Calculated in accordance with what was reported in Ref. [20].
[b] Calculated in accordance with what was reported in Ref. [19].

microcomputer processing using MILES-200 and MILEADP software for computations. Prior to the analysis, the calcined samples were outgassed at 623 K (*ca.* 16 h) under vacuum (10^{-2} mbar).

Temperature-programmed reduction (TPR) experiments were carried out with a TPDRO-1100 (CE Instruments) equipped with a quartz glass reactor with a porous septum (*ca.* 8 mm i.d.) and a filter filled with soda lime for trapping acid gases and water. Prior to the TPR runs, the samples were heated in a stream of O_2/N_2 (20% v/v, flowing at 14 cm^3/min) ramping the temperature at 10 K/min from room temperature to 673 K and maintaining it for 90 min, and then cooling at 313 K in static atmosphere of O_2/N_2. TPR measurements were carried out using 4.98 vol% hydrogen in argon as a reducing gas. The gas flow rate was adjusted by mass flow controllers to 14 cm^3/min with a thermal conductivity detector (TCD) for measuring the amount of H_2 uptake. A heating rate of 10 K/min from 313 to 800 K was used for all the measurements. Peak areas were calibrated employing CuO bulk standard per analysis as reference material or pure H_2 (Sapio, Italy; purity >99.9999%) injections. Typical sample size used was about 55 mg of sample corresponding to amounts of CuO in the range from 27 to 150 μmol depending on the Cu loading (table 2).

2.3. Catalytic tests

The catalytic activity in the reduction of NO by C_2H_4 in oxygen-rich atmosphere was determined in a fixed-bed quartz reactor. Experimental details have been presented in Ref. [35]. A typical gas feed consisted of 4000 ppm of both NO and C_2H_4 and of 40 000 ppm of O_2 in helium. Reaction was investigated at different temperatures (423–773 K) and space velocities (7500–15 000 h^{-1}). The reactor outflow was analyzed using a gas chromatograph (Chrompack, CP-9000) equipped with a TCD detector and a 60/80 Carboxen-1000 column (Supelchem 3.2 mm × 4.6 m stainless steel) for the separation of O_2, N_2, NO, N_2O, CO, CO_2, and C_2H_4.

3. Results and discussion

3.1. Catalyst characterization

It is known that the support crystalline matrix chosen for this study has microporous characteristics: higher internal than external surface (480 and 43 m^2/g, respectively) and monomodal distribution in the range of micropores (4–5 Å of pore radius) [16]. The ETS-10 matrix was loaded with copper amounts deposited by ion-exchange procedure for samples containing from 3 to 11 wt% Cu and by ion exchange plus impregnation of copper salt precursor procedures for samples containing from 15 to 18 wt% Cu (see table 1). The first series of samples are underexchanged materials with copper concentration from 0.7 to 3.5 Cu-atoms per surface unity (table 1). The second series of samples are overexchanged materials with Cu concentration from 30 to 70 $atom_{Cu}\,nm^{-2}$. The tremendous increase of copper concentration is due to the increase of Cu loading and mainly to the abrupt drop of surface area observed for samples loaded with more than 11 wt% Cu. The high Cu loading led to structure collapse of the support matrix with formation of CuO agglomerates of 250–350 nm size, calculated on the basis of the broadening of the CuO X-ray peaks (2θ values in the 36–39° region). On the other hand, the low-copper-containing catalysts showed XRD patterns indistinguishable from that of the parent matrix. The crystalline structures remained practically unperturbed by the copper exchange procedure and no peak related to bulky CuO was found, suggesting that copper species in the ETS-10 matrix can be atomically dispersed.

The contribution of the internal surface area to the total surface area of ETS-10 was about 90% with 0.15 cm^3/g of micropore volume. The deposition of increasing amounts of copper (from 3 to 8 wt%) on ETS-10 caused a slight decrease (about 20%) of the internal surface area (350 m^2/g and 0.125 cm^3/g), whereas the external surface area was only slightly affected. A more important loss of internal surface area (about 40%) was observed for the catalyst containing 11 wt% Cu (240 m^2/g with 0.08 cm^3/g) with a slight increase of the external surface (60 m^2/g). For higher Cu deposition, the samples did not have any internal surface area. Structure collapse of the matrix was observed and it was responsible for the complete loss of microporous surface area. The ETS-10 matrix cannot admit such a high amount of copper. The high proportion of voids in ETS-10 makes it a weak point of the structure from a mechanical point of view, so it is unable to sustain high amounts of copper. The trend of the total surface area of copper catalysts as a function of copper concentration is reported in figure 1. A well-defined plateau can be observed up to about 2.5 $atom_{Cu}\,nm^{-2}$. At increasing copper concentration, an abrupt decrease of surface area is observed. Due to the low copper loading and

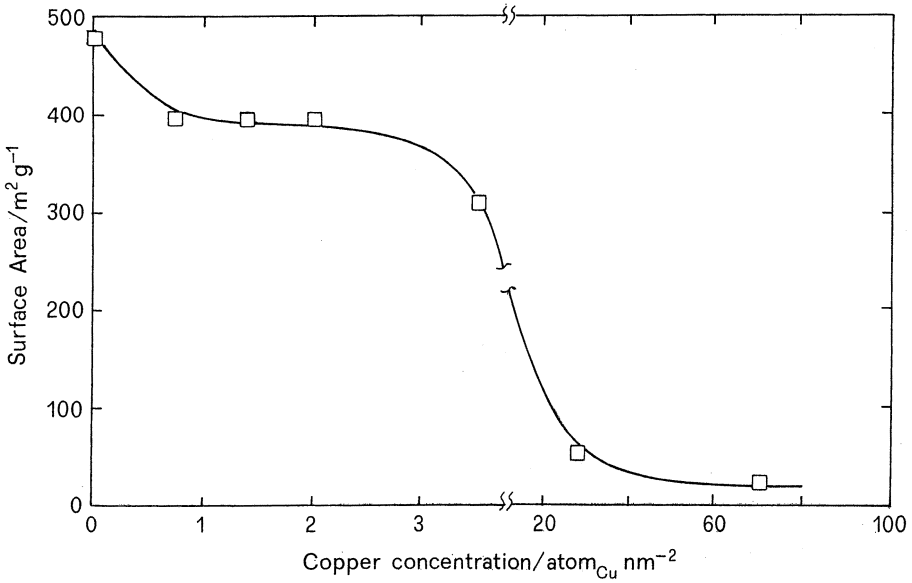

Figure 1. Surface area of the catalysts as a function of copper concentration.

the wide surface disposable, the series of catalysts at low copper content (up to 2.5 $atom_{Cu}\,nm^{-2}$) should contain highly dispersed copper species.

3.1.1. Reduction behavior

The reduction behavior of CuO_x in the Cu-ETS-10 catalysts was studied by temperature-programmed reduction (TPR). The experimental operating conditions have been selected in order to obtain unperturbed reduction profiles [36,37]. The characteristic value K ($K = S_0/VC_0$, where S_0 is the initial amount of reducible CuO, in mol, V is the total flow rate, in cm^3/min, and C_0 is the initial hydrogen concentration in the feed, in mol/cm^3) ranges from 55 to 150 s [38,39]. The sensitivity becomes too low when working with excessively low K values; however, loss of linear concentration profile can result for too high values of K. Moreover, the P parameter, defined as βK with β the increasing temperature rate, should be suitably chosen [40]. As the amount of CuO (S_0) in the studied catalysts was in a wide range, it was not possible to perform the reductions with unique K and P values. Experiments were done maintaining constant the mass of the different samples, leading to K values ranging from about 50 to 160 s and P values from about 5 to 30 K (table 2). This choice was made because a five-times higher amount of the sample with the lowest copper concentration than the amount of that with the highest copper concentration would have been necessary to obtain the same value of $K = 150$. On the other hand, an excessive amount of powder in the TPR reactor leads to problems of pressure drop that influence the response of the TCD detector too much.

As shown in figure 2, the areas of the TPR peaks increased from Cu02-ETS-10 to Cu3-ETS-10 due to the increasing copper amount per unit mass. Besides the peak area, the increasing of Cu amount influences the shape of the TPR peak. Two reduction peaks with maximum temperatures at *ca.* 470 K ($T_{m,1}$) and at *ca.* 560 K ($T_{m,2}$) were clearly observed (table 3) for catalysts with copper concentration up to 3.5 $atom_{Cu}\,nm^{-2}$. Catalysts containing copper at higher concentration had only the high-temperature reduction peak.

Bulk CuO has the reduction peak at temperature higher (*ca.* 700 K) than all the tested samples. The two reduction peaks could be explained by stepwise reductions of the CuO_x phase, from Cu(II) to Cu(I) and then to Cu(0), or by single-stage reduction, from Cu(II) to Cu(0), of two different types of Cu(II) species [41]. The former hypothesis cannot hold, because the areas of the two peaks were too different, while the co-presence of copper oxide species at different nuclearity can be responsible for the complex reduction profile observed. The most significant feature of the TPR profiles of catalysts is the presence of the low-temperature reduction peak for the catalysts with low copper concentration (up to 2 $atom_{Cu}\,nm^{-2}$) as compared with those highly loaded. These catalysts display only one well-resolved peak at higher temperature, and only the occurrence of a shoulder at the position of the low-temperature reduction peak was observed for Cu1-ETS-10. Large particles of CuO_x at high nuclearity may be expected to reduce in a similar manner to unsupported oxide, the matrix acting merely as a dispersing agent [42,43]. Under these conditions the reduction kinetics observed for the highly loaded copper catalysts resembles that found for bulk CuO.

It can be concluded that the interaction of small aggregates of CuO_x species with the ETS-10 matrix has an effect in the lowering of the reduction temperatures of the dispersed copper species. Referring to the

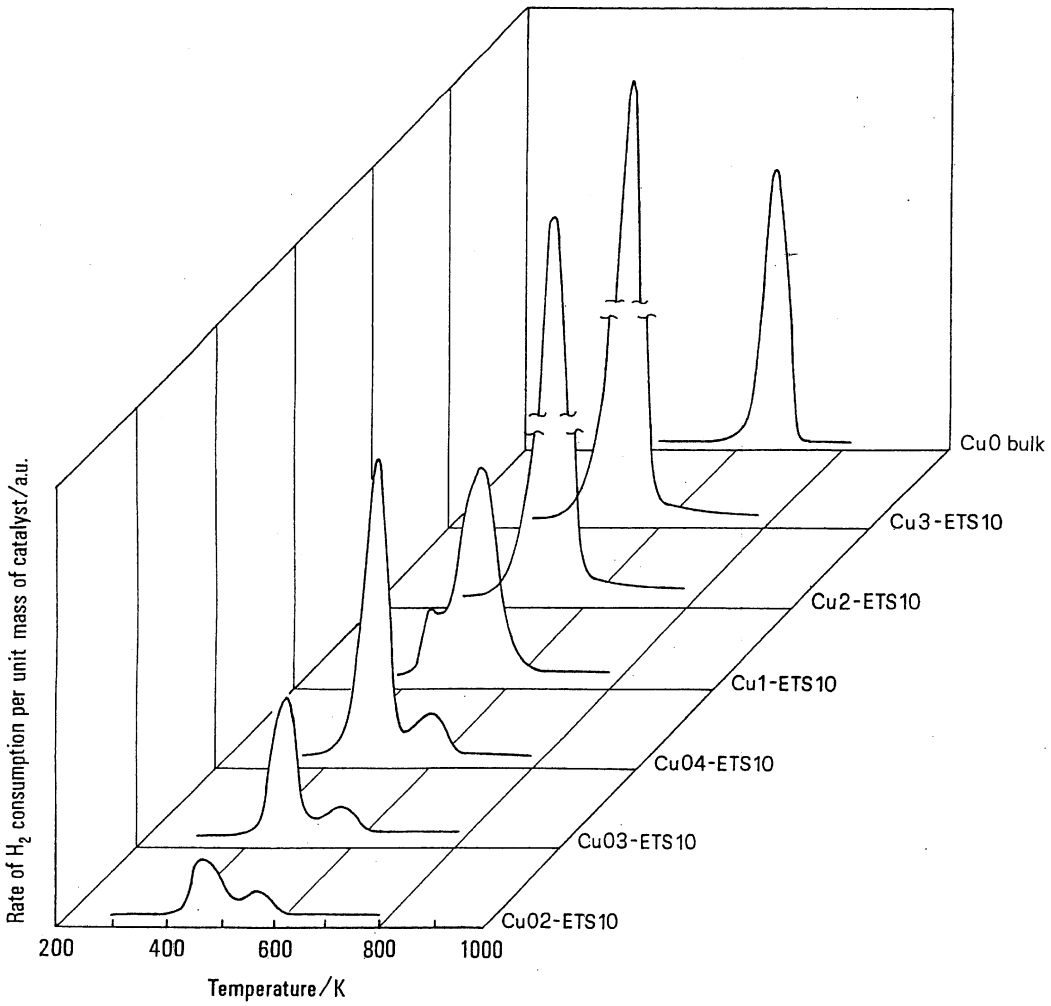

Figure 2. TPR profiles for the reduction of CuO_x on ETS-10-based catalysts. Reduction of bulk CuO has been used as reference.

literature [19,23,42,43], it seems reasonable to suggest that the low- and high-temperature peaks correspond to the reduction of highly dispersed and non-interacting CuO_x species and of crystalline CuO_x species, respectively. To verify this argument, the areas of the two reduction peaks have been calculated, as percentages of total hydrogen uptake, and reported in table 3. A better visualization of H_2 consumed for the two peaks distinctly against the copper concentration of the catalysts is displayed in figure 3. The low-temperature peak area, which is supposed to be proportional to the amount of highly dispersed CuO_x species, increases

Table 3
TPR experimental results of the studied copper ETS-10 materials.

Sample	Peak maximum temperature		Peak area		Reduction (%)
	$T_{m,1}$ (K)	$T_{m,2}$ (K)	A_1 (%)[a]	A_2 (%)[a]	
ETS-10	–	–	–	–	–
Cu02-ETS-10	462	572	71.53	28.47	97[b]
Cu03-ETS-10	479	582	78.77	21.23	96[b]
Cu04-ETS-10	502	608	83.90	16.10	115[b,c]
Cu1-ETS-10	455	555	11.14	88.86	90[b,c]
Cu2-ETS-10	–	547	–	100	108[c]
Cu3-ETS-10	–	556	–	100	115[c]

[a] Areas of peaks 1 and 2 as percentage of total uptake.
[b] Determined employing CuO bulk standard per analysis as reference material.
[c] Determined employing H_2 injection in H_2/Ar 5% v/v carrier as reference (from 0.01 to 0.3 ml).

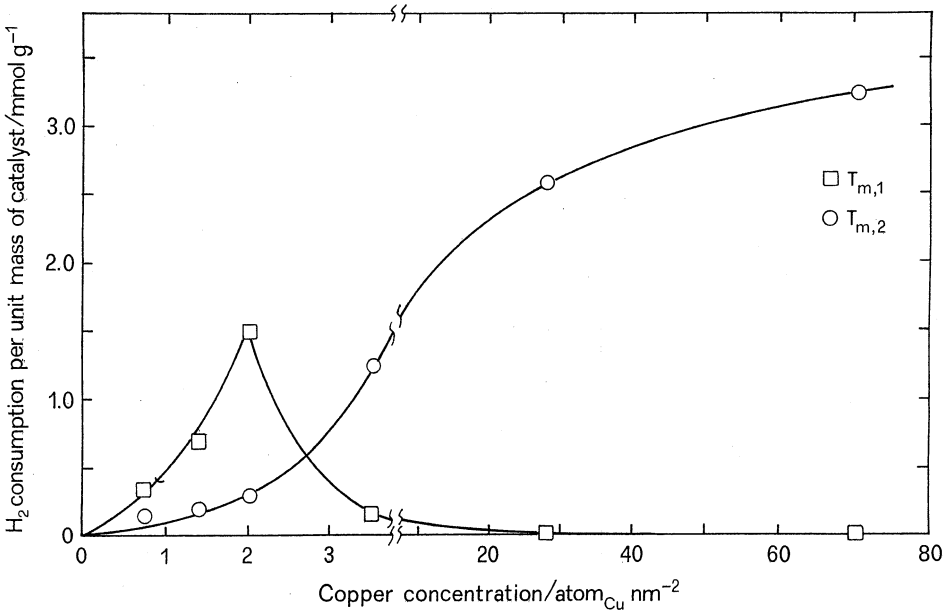

Figure 3. Contribution of the low-temperature ($T_{m,1}$) and of the high-temperature ($T_{m,2}$) reduction peaks to the total hydrogen consumption for each catalyst as a function of copper concentration.

rapidly, attaining a maximum (at 2 $atom_{Cu}\,nm^{-2}$), and then rapidly falls down. The high-temperature reduction peak has a pronounced sigmoidal shape. The two curves intersect at about 2.5–3 $atom_{Cu}\,nm^{-2}$. This is basically consistent with the maximum dispersion capacity of CuO_x on the ETS-10 matrix, in accordance with the above-reported evidence. It is interesting to observe that both the maximum temperatures of reduction of the two peaks ($T_{m,1}$ and $T_{m,2}$) have an increasing trend up to Cu04-ETS-10 (2 $atom_{Cu}\,nm^{-2}$) and then decrease when viewed as a function of copper concentration (table 3). This behavior suggests that the reduction process could be perturbed by sublimation phenomena of copper species [40]. With catalysts at low copper content, at the beginning of the reduction very small particles of metallic copper are formed because the sintering is hampered by the good dispersion and isolation of the CuO_x species. As the TPR run proceeds, these small particles of metallic copper could have enough energy to sublime, thus covering the unreduced CuO_x species. The reduction of the CuO_x phase is probably hindered by the metallic copper film, the hydrogen having to diffuse through it before reacting with the CuO_x species, thus leading to an increase of the observed $T_{m,1}$ and $T_{m,2}$ temperatures from Cu02- to Cu04-ETS-10. When the copper loading becomes high enough, sublimation can be avoided.

The percentages of reduction, calculated from the sum of the two reduction peaks, were in all cases close to 100% (table 3, column 6). This demonstrates that all the CuO_x species constitute an easily reducible phase, independently of the extension of the aggregates formed. Due to the wide range of copper content in the catalysts, the absolute values of the peak areas of the various catalysts were different by some orders of magnitude. For this reason, peak areas were calibrated by injecting pure hydrogen pulses of known volume (for samples at high Cu content) or by employing pure CuO bulk standard (for samples at low Cu content) depending on the amount of copper in the catalyst.

3.2. Catalytic activity in the C_2H_4-SCR of NO

The copper samples based on ETS-10 were tested with the reduction of NO by ethylene in oxidizing atmosphere ($NO–C_2H_4–O_2$). Ethylene was chosen as the reducing species toward NO in response to the fact that it is presently the most prevalent hydrocarbon in exhaust gases from gasoline engines. The sensitivity of C_2H_4-SCR activity of the catalysts to varying temperatures and space velocities was also studied. Significant differences emerged between the low- and the high-copper-loaded catalysts in terms of catalytic activity, N_2 production, and selectivity [5,16]. The catalysts with copper concentration higher than 3.5 $atom_{Cu}\,nm^{-2}$ did not produce any N_2, while those with lower copper concentration were active and selective to the N_2 production.

As a general trend, the $NO–C_2H_4–O_2$ reaction followed the same pattern for all the catalysts: the reduction of NO began at the same time as the oxidation of C_2H_4, between 473 and 523 K. For increasing temperatures, the N_2 formation increased, up to 573 K, and then decreased in a more or less marked way depending on the sample, while ethylene oxidation attained and maintained its maximum value. Among the active catalysts (Cu02-, Cu03-, Cu04-, and Cu1-ETS-10), the NO percentage conversion was not substantially different (*ca.* 25%).

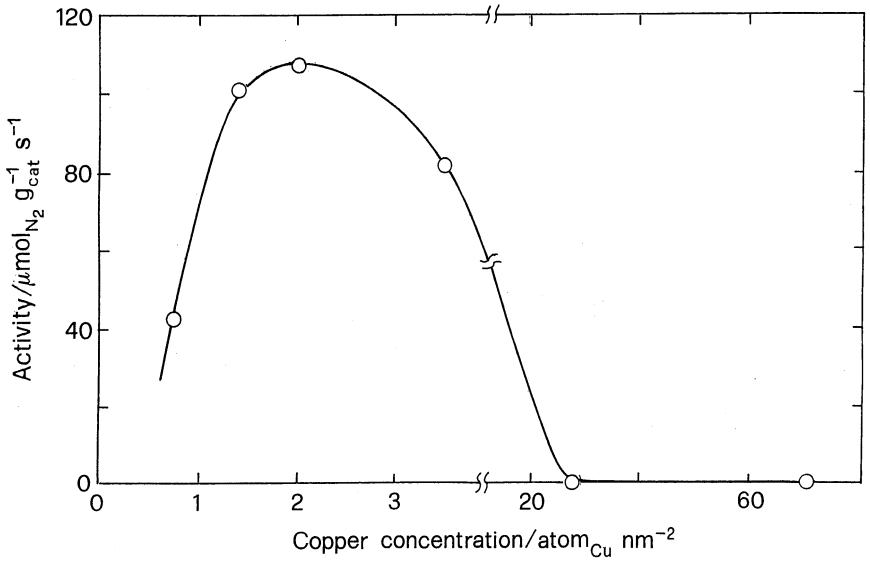

Figure 4. Specific activity of NO reduction to N_2 in oxygen (expressed as $\mu mol_{N_2}\ g_{cat}^{-1}\ s^{-1}$) at 573 K as a function of copper concentration.

The only significant difference was observed for Cu02-ETS-10 that had a volcano-shaped curve of NO conversion shifted at higher temperature than the other catalysts, with maximum at 723 K instead of 598–623 K. A clear increasing trend was observed for ethylene conversion to CO_2, the conversion increasing in the following order: Cu02-, Cu03-, Cu04-, and Cu1-ETS-10. At 623 K, CO_2 formation was 61, 79, 97, and 100% for Cu02-, Cu03-, Cu04-, and Cu1-ETS-10, respectively.

The specific activity of N_2 formation of the catalysts as a function of copper concentration is displayed in figure 4. At first, an increasing trend with the copper concentration up to 2 atom$_{Cu}$ nm^{-2} followed by a decrease down to zero for copper concentration around 20 atom$_{Cu}$ nm^{-2} was observed. The plot has been drawn with the results obtained at 573 K of reaction temperature. The trend with the maximum at about 2.5 atom$_{Cu}$ nm^{-2} suggests that not all the copper deposited on the matrix is active, but only the highly dispersed copper fraction could be associated with active sites.

The catalytic results obtained over the copper catalysts in the 423–773 K range could be rewritten in terms of logarithm of turnover frequency per copper site (mole of NO converted to N_2 per mole of copper site per unit time) against the inverse of temperature giving rise to an Arrhenius-like plot (figure 5). Linear trends were observed for all the catalysts. The position of the lines reflects the activity of each catalyst:

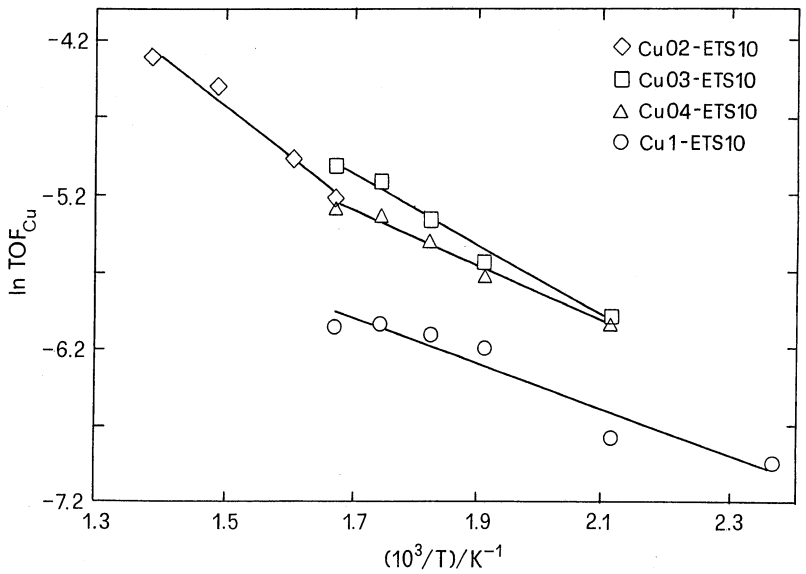

Figure 5. Arrhenius-like plot expressed as turnover frequencies (NO molecules converted to N_2 min^{-1} Cu-atoms^{-1}) for NO abatement with C_2H_4 in oxygen over copper ETS-10 catalysts. Feed: NO and $C_2H_4 = 0.4\%$ v/v and $O_2 = 4\%$ v/v.

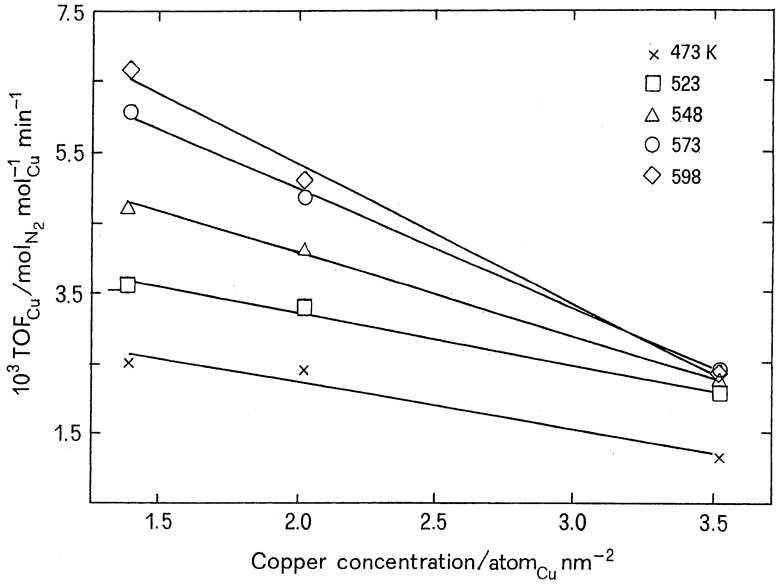

Figure 6. Turnover frequencies (NO molecules converted to $N_2\,min^{-1}$ Cu-atoms^{-1}) for NO reduction with C_2H_4 in oxygen as a function of copper concentration for different temperatures. Feed: NO and $C_2H_4 = 0.4\%$ v/v and $O_2 = 4\%$ v/v.

Cu03-ETS-10 lies over Cu04-ETS-10, and this one over Cu1-ETS-10. The line for Cu02-ETS-10 is shifted at higher temperature, as reported above.

The amount of copper deposited on the ETS-10 matrix affects the activity of the NO reduction. Figure 6 shows the turnover frequency per copper site calculated at various temperatures as a function of copper concentration. A clear decreasing trend can be observed starting from $0.7\,atom_{Cu}\,nm^{-2}$ (Cu02-ETS-10) to $3.5\,atom_{Cu}\,nm^{-2}$ (Cu1-ETS-10). The slope of each line increases with temperature. For lower values of copper concentration, it is possible to observe an important positive effect of temperature on the SCR activity, while for higher values of copper concentration it is not possible to observe a clear influence of temperature. This behavior is due to the presence of large aggregates of CuO_x on the more concentrated catalysts that possess oxidation activity towards ethylene besides SCR activity, in accordance with what was proposed by Chajar *et al.* [31].

Cu1-ETS-10 has been chosen from the studied catalysts to perform a detailed kinetic study on the C_2H_4-SCR of NO reaction. Experimental data have been collected at various contact times from 0.72 to 0.14 s for different temperatures (from 523 to 673 K), maintaining the feed concentration at a constant level (0.4% of NO and C_2H_4 and 4% of O_2). Table 4 summarizes the more significant results in terms of N-products (N_2 and N_2O) and C-products (CO_2 and CO) obtained. Selectivity to SCR has been also calculated as a competitive factor (c.f.), that is, the amount of C_2H_4 consumed to reduce NO with respect to the total amount of C_2H_4 consumed [34,35]. At any time, the c.f. values decreased as temperature increased, because C_2H_4 oxidation by O_2 prevailed on C_2H_4 oxidation by NO, as expected [35]. The typical volcano-shaped curve for the N_2 formation against temperature was clearly observed for contact times between 7500 and 15 000 s^{-1}. For higher or lower contact times, the N_2 species was decreasing with temperature. No clear trend was observed for the N_2O species, which remained almost constant independently of time and temperature. Complete conversion of C_2H_4 was observed at various times but it was attained at higher temperature by decreasing the contact time.

The data collected in table 4 were utilized for a kinetic study aimed at quantifying the ability of the copper sites

Table 4
Catalytic activity in the NO–C_2H_4–O_2 reaction of Cu1-ETS-10 for runs at different contact times [and selected reaction temperatures (T_R)[a]].

Contact time[b] (s)	T_R (K)	Y_{N_2} (%)	Y_{N_2O} (%)	Y_{CO_2} (%)	Y_{CO} (%)	c.f.
0.72 (5000)	523	24.75	16.51	61.96	–	6.66
	573	19.23	16.98	100	–	3.19
	623	15.86	16.26	100	–	2.59
	673	11.46	16.28	100	–	1.86
0.48 (7500)	523	19.26	18.22	50.05	–	6.42
	573	23.44	18.05	94.57	–	3.95
	623	20.84	17.55	100	–	3.32
	673	18.55	16.52	100	–	2.94
0.24 (15 000)	523	15.34	15.19	24.90	–	10.26
	573	16.93	19.12	73.60	–	3.83
	623	15.17	18.57	98.56	–	2.57
	673	7.95	18.81	100	–	1.29
0.14 (25 000)	523	–	–	20.50	–	–
	573	11.43	–	58.00	–	3.26
	623	10.11	–	87.72	–	1.92
	673	–	–	98.48	–	–

[a] Feed concentration: NO and C_2H_4, 0.4% v/v; and O_2, 4% v/v.
[b] Values in parentheses represent space velocity (h^{-1}, GHSV).

to oxidize C_2H_4 by NO rather than by O_2. The overall reaction can be viewed, for a simplified kinetic interpretation, as a combination of simultaneous competitive reactions [35,44], in accordance with the following scheme:

$$6NO + C_2H_4 \xrightarrow{k_1} 3N_2 + 2CO_2 + 2H_2O \quad (1)$$

$$3O_2 + C_2H_4 \xrightarrow{k_2} 2CO_2 + 2H_2O \quad (2)$$

$$8NO + C_2H_4 \xrightarrow{k_3} 4N_2O + 2CO + 2H_2O \quad (3)$$

$$2O_2 + C_2H_4 \xrightarrow{k_4} 2CO + 2H_2O. \quad (4)$$

In this scheme, the formation of NO_2 species has been ruled out due to the very minor activity of copper-based catalysts to NO_2 formation [45,46]. The four reactions run at different rates and possess different activation parameters. The coefficients k_1 and k_3 are the rate constants of the reactions associated with the NO reduction activity of the catalysts, and k_2 and k_4 are those associated with the oxidation activity by O_2.

Considering altogether the NO reduction products, N_2 and N_2O, as well as the oxidation products, CO_2 and CO (if present), it is possible to write the following equations:

$$\frac{d(P_{N_2} + P_{N_2O})}{dt} = 3r_1 + 4r_3 \quad (5)$$

$$\frac{d(P_{CO_2} + P_{CO})}{dt} = 2(r_1 + r_2 + r_3 + r_4) \quad (6)$$

$$\frac{d(P_{N_2} + P_{N_2O})}{d(P_{CO_2} + P_{CO})} = \frac{3r_1 + 4r_3}{2(r_1 + r_2 + r_3 + r_4)} \quad (7)$$

where P_i indicates the partial pressure of the ith species, and r_1, r_2, r_3, and r_4 indicate the rates of C_2H_4 consumption in reactions (1), (2), (3), and (4) respectively.

On the basis of the procedure detailed in Ref. [35], which describes the variation in the amount of N_2 and N_2O with respect to CO_2 (and CO, if present), it is possible to calculate the rate-constant ratio $R_k = (k_2 + k_4)/(k_1 + k_3)$. The most probable value of R_k at each temperature was obtained by means of a computer program which employed the optimization subroutine VA04A [47] to minimize the following objective function:

$$\Phi = \left\{ \sum_{i=1}^{n} \frac{[(P_{N_2} + P_{N_2O})_{exptl} - (P_{N_2} + P_{N_2O})_{calcd}]^2}{n-1} \right\}^{1/2} \quad (8)$$

where the $(P_{N_2} + P_{N_2O})_{exptl}$ are the experimental amounts of N_2 and N_2O formed at a given contact time, n is the number of different contact times employed, and $(P_{N_2} + P_{N_2O})_{calcd}$ are the calculated amounts of N_2 and N_2O. The values of $(P_{N2} + P_{N2O})$ for any value of $(P_{CO_2} + P_{CO})$ were calculated by the computer program by numerical integration starting from equation (7). The numerical integration was performed through a fourth-order Runge–Kutta method [48].

The R_k values obtained at the various temperatures, ranging from 0.6 at 523 K to 2.2 at 673 K, reported in an Arrhenius-type plot ($\ln R_k$ *versus* $1/T$) gave a satisfactory linear trend as shown in figure 7. The slope of the calculated line ($\Delta E_a/R$) permits obtaining a rough estimate of the difference between the activation energy of the oxidation of C_2H_4 by O_2 (considering the reactions (2) and (4) together) and that of the reduction of NO by C_2H_4 (considering the reactions (1) and (3) together):

$$\Delta E_a = E_{a,O_2} - E_{a,NO}.$$

The numerical value of this difference was found to be $24.9 \pm 0.98\ kJ\ mol^{-1}$. Thus, the reaction of C_2H_4 oxidation by O_2 showed an activation energy much higher than those of C_2H_4 by NO. This is in agreement with the experimental evidence reported above and

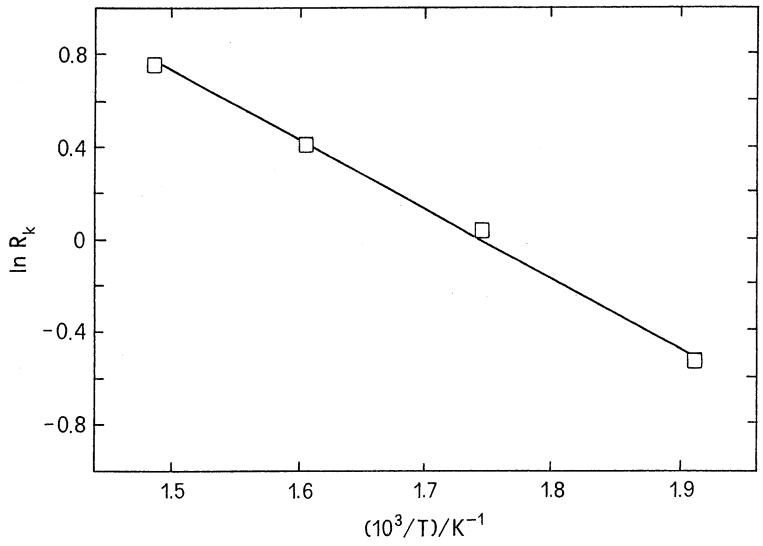

Figure 7. Arrhenius-type plot for the NO reduction with C_2H_4 in oxygen over the Cu1-ETS-10 catalyst. $R_k = (k_2 + k_4)/(k_1 + k_3)$.

with previous results obtained on $Cu/SiO_2–Al_2O_3$ catalysts [35]. The oxidation of C_2H_4 was mainly due to NO for temperatures up to 523–573 K, while at higher temperatures the reactions in which the oxidation reagent is O_2 were abruptly started.

4. Conclusions

On the series of catalysts prepared by loading copper oxide on ETS-10, the physico-chemical and reductive properties as well as the catalytic activity of NO reduction follow a trend which is related to the dispersion of the CuO_x species.

The very strong influence of the number of CuO_x dispersed species in the SCR of NO has been confirmed. The existence of an isolated CuO_x-like phase is a direct consequence of the matrix acting as a dispersing agent. The double charge on octahedrally coordinated Ti atoms in ETS-10 may create a high negative framework charge, which results in a stronger electrostatic interaction with the copper species.

Acknowledgments

Support from MURST-2000, coordinator V. Indovina, is gratefully acknowledged. The authors wish to thank V. Modica for the experimental contribution.

References

[1] M. Iwamoto and H. Hamada, Catal. Today 10 (1991) 57.
[2] M. Iwamoto, H. Yahiro, S. Shundo, Y. Yu-u and N. Mizuno, Appl. Catal. 69 (1991) L15.
[3] S. Sato, Y. Yu-u, H. Yahiro, N. Mizuno and M. Iwamoto, Appl. Catal. 70 (1991) L1.
[4] M. Shelef, Chem. Rev. 95 (1995) 209.
[5] Y. Traa, B. Burger and J. Weitkamp, Micropor. Mesopor. Mater. 30 (1999) 3.
[6] H.H. Kung and M.C. Kung, Catal. Today 30 (1996) 5.
[7] M. Iwamoto, H. Furukawa, Y. Mine, G. Mikuriya and S. Kagawa, J. Chem. Soc., Chem. Commun. (1986) 1272.
[8] A. Corma, V. Fornés and E. Palomares, Appl. Catal. B 11 (1997) 233.
[9] B. Coq, D. Tachon, F. Figuéras, G. Mabilon and M. Prigent, Appl. Catal. B 6 (1995) 271.
[10] W. Li, M. Sirilumpen and R.T. Yang, Appl. Catal. B 11 (1997) 347.
[11] T. Ishihara, M. Kagawa, F. Hadama and Y. Takita, J. Catal. 169 (1997) 93.
[12] O. Okada, T. Tabata, M. Kokitsu, H. Ohtsuka, L.M.F. Sabatino and G. Bellussi, Appl. Surf. Sci. 121/122 (1997) 267.
[13] M.W. Anderson, O. Tesaraki, T. Ohsuna, A. Philippou, S.P. MacKay, A. Ferreira, J. Rocha and S. Lidin, Nature 367 (1994) 347.
[14] R.J. Saxton, Topics Catal. 9 (1999) 43.
[15] A. Auroux, C. Picciau and A. Gervasini in: *Studies in Surface Science and Catalysis* (Elsevier, Amsterdam, 1999), vol. 125, p. 555.
[16] A. Gervasini, C. Picciau and A. Auroux, Micropor. Mesopor. Mater. 35–36 (2000) 457.
[17] S. Bordiga, C. Pazé, G. Berlier, D. Scarano, G. Spoto, A. Zecchina and C. Lamberti, Catal. Today 70 (2001) 91.
[18] T. Cheung, S.K. Bhargava, M. Hobday and K. Foger, J. Catal. 158 (1996) 301.
[19] C. Torre-Abreu, M.F. Ribeiro, C. Henriques and G. Delahay, Appl. Catal. B 12 (1997) 249.
[20] T. Beutel, J. Sárkány, G.-D. Lei, J.Y. Yan and W.M.H. Sachtler, J. Phys. Chem. 100 (1996) 845.
[21] C. Dossi, A. Fusi, S. Recchia, R. Psaro and G. Moretti, Micropor. Mesopor. Mater. 30 (1999) 165.
[22] G. Moretti, C. Dossi, A. Fusi, S. Recchia and R. Psaro, Appl. Catal. B 20 (1999) 67.
[23] R. Bulánek, B. Wichterlová, Z. Sobalík and J. Tichy, Appl. Catal. B 31 (2001) 13.
[24] M.C.N. Amorim de Carvalho, F.B. Passos and M. Schmal, Appl. Catal. A 193 (2000) 265.
[25] Dedeček, Z. Sobalik, Z. Tvarůžková, D. Kaucký and B. Wichterlová, J. Phys. Chem. 99 (1995) 16327.
[26] C. Henriques, M.F. Ribeiro, C. Abreu, D.M. Murphy, F. Poignant, J. Saussey and J.C. Lavalley, Appl. Catal. B 16 (1998) 79.
[27] S.-K. Park, V. Kurshev, Z. Luan, C.W. Lee and L. Kevan, Micropor. Mesopor. Mater. 38 (2000) 255.
[28] B. Coq, D. Tachon, F. Figuéras, G. Mabilon and M. Prigent, Appl. Catal. B 6 (1995) 271.
[29] C. Torre-Abreu, M.F. Ribeiro, C. Henriques and F.R. Ribeiro, Appl. Catal. B 11 (1997) 383.
[30] C. Márquez-Alvarez, I. Rodríguez-Ramos, A. Guerrero-Ruiz, G.L. Haller and M. Fernández-García, J. Am. Chem. Soc. 119 (1997) 2905.
[31] Z. Chajar, M. Primet and H. Praliaud, J. Catal. 180 (1998) 279.
[32] D. Pietrogiacomi, D. Sannino, S. Tuti, P. Ciambelli, V. Indovina, M. Occhiuzzi and F. Pepe, Appl. Catal. B 21 (1999) 141.
[33] G. Centi, S. Perathoner, D. Biglino and E. Giamello, J. Catal. 152 (1995) 75.
[34] K.A. Bethke, M.C. Kung, B. Yang, M. Shah, D. Alt, C. Li and H.H. Kung, Catal. Today 26 (1995) 169.
[35] P. Carniti, A. Gervasini, V.H. Modica, N. Ravasio, Appl. Catal. B 28 (2000) 175.
[36] B. Jouguet, A. Gervasini and A. Auroux, Chem. Eng. Technol. 18 (1995) 243.
[37] M. Fadoni and L. Lucarelli, Stud. Surf. Sci. Catal. 120A (1999) 177.
[38] P. Malet and A. Caballero, J. Chem. Soc., Faraday Trans. I 84(7) (1988) 2369.
[39] D.A.M. Monti and A. Baiker, J. Catal. 83 (1983) 323.
[40] G. Fierro, M. Lo Jacono, M. Inversi, P. Porta, R. Lavecchia and F. Cioci, J. Catal. 148 (1994) 709.
[41] G.C. Bond, S.N. Namijo and J.S. Wakeman, J. Mol. Catal. 64 (1991) 305.
[42] G. Córdoba, M. Viniegra, J.L.G. Fierro, J. Padilla and R. Arroyo, J. Solid State Chem. 138 (1998) 1.
[43] F.S. Delk and A. Vãvere, J. Catal. 85 (1984) 380.
[44] P. Carniti and A. Gervasini, React. Kinet. Catal. Lett. 67 (1999) 233.
[45] M. Shelef, C.N. Montreuil and H.W. Jen, Catal. Lett. 26 (1994) 277.
[46] V. Tomašic, Z. Gomzi and S. Zrncevic, Appl. Catal. B 18 (1998) 233.
[47] M.J.D. Powell, Comput. J. 7 (1965) 303.
[48] B. Carnahan, H.A. Luther and J.O. Wilkes, *Applied Numerical Methods* (Wiley, New York, 1969), p. 361.